A Fatigue State Evaluation System Based on the Band Energy of Electroencephalography Signals

Chin-Shun Hsieh* and Cheng-Chi Tai

Department of Electrical Engineering, National Cheng Kung University,
Tainan City 70101, Taiwan, R.O.C.

Cranial nerve information can be used to correctly analyze fatigue states. Spectral analysis is the major method of identifying fatigue states. Various frequency bands can be distinguished by digital filters owing to their high accuracy and driftless features. The electroencephalography (EEG) signal is sent to a personal computer (PC) via a universal serial bus (USB) interface from a microcontroller and passed through digital filters within 200 taps, and thus, the spectrum of individual signals can be analyzed. This study has investigated the four EEG frequency bands, delta (δ), theta (θ), alpha (α), and beta (β), using four algorithms to evaluate the fatigue state based on the EEG signals. We compared the four algorithms and determined the best one.

1. Introduction

Mood incompetence may hinder or even endanger human life, particularly for those designated to make important decisions, operate dangerous tools, or cope with emergency situations (pilots, truck drivers, emergency room staff, just to name a few). In this study, we detect a person's state of mind. Horne and Baulk[1] have arranged two sessions on a driving simulator and tested the subjects. They found a very high correlation between Karolinska Sleepiness Scale (KSS) scores and power of 4–11 Hz band ($\theta+\alpha$ band), and therefore, can take advantage of the band energy to assess their sleepiness states (KSS scores) in real time.

In the study of Akerstedt and Gillberg,[2] which considers relationships between subjective sleepiness and EEG, subjects were kept awake during the night in the laboratory. A high sleepiness condition was related to an increase in theta and alpha power.

Subjective sleepiness correlates negatively with global α (8–12 Hz) and positively with central frontal θ (4–8 Hz) frequencies in the human resting awake electroencephalo gram.[3,4]

---

*Corresponding author: e-mail: sjs1@hhvs.tnc.edu.tw

In another study on anxiety, self-reports were made by means of the Hamilton Anxiety Scale (HAS). HAS (or HAMA) is a 14-item test measuring the severity of anxiety symptoms. It is also sometimes called the Hamilton Anxiety Rating Scale (HARS).[5] HAS is used to evaluate the severity of anxiety symptoms observed in children and adults. It is also used as an outcome measurement when evaluating the impact of anti-anxiety medications and remedies and is a standard measurement of anxiety used in evaluations of psychotropic drugs.

A significant relationship between reported anxiety and β2 power over midline electrodes (Fz, Cz and Pz are shown in Fig. 1) was described by Ansseau *et al.*[6] The letters F, T, C, P, and O stand for frontal, temporal, central, parietal, and occipital lobes, respectively. A "z" (zero) refers to an electrode placed on the midline. The results showed a significantly more rapid onset of activity of freeze-dried dosage formulation (FDDF) of oxazepam for anxiety level ($p < 0.005$) and the specific β2 EEG changes ($p < 0.0001$), which were significantly correlated ($r = -0.73$, r is coefficient of correlation; $p < 0.01$, p is probability).

EEG activity sources were analyzed using the low-resolution electromagnetic tomography (LORETA) method (Isotani *et al.*[7]). The β2 activity source was found to move to the right side during anxiety conditions in comparison with relaxation conditions. The reports agree that brain activity shifts to the right (especially frontotemporal) during negative emotions (compared with positive emotions), and support the role of β2 EEG frequency in emotional states.

Figure 1 shows how the electrodes are placed. For example, the overuse of smart phones leads to anxiety. β rhythm (β wave band) is noted under conditions of mood effort and also during emotional arousal, which in some conditions can have negative valence. α rhythm is positively correlated with the awake state of relaxation, which has emotionally positive valence and is opposite of tense arousal.[8]

Since the interval frequency of brain wave composition is very close to the neighboring band, digital filtering is required. The current study has investigated the
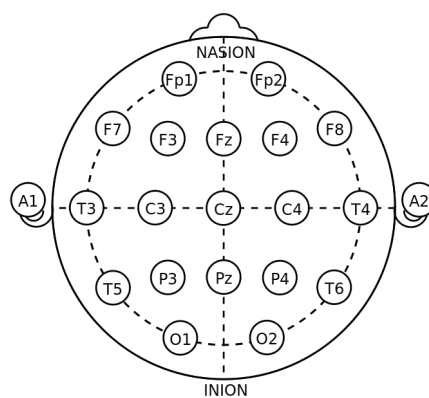

Fig. 1.   10–20 system for electrode placement (from Wikipedia).

four EEG frequency bands, δ, θ, α, and β, using four algorithms (algorithm 1 = $(\theta+\alpha)/\beta$, Brookhuis & Waard;[9] algorithm 2 = α/β, Eoh *et al.*;[10] algorithm 3 = $(\theta+\alpha)/(\alpha+\beta)$, and algorithm 4 = θ/β, Budi *et al.*[11]) to evaluate fatigue. For example, the α (α1, 8–10 Hz; α2, 10–12 Hz), β (β1, 13–15 Hz; β2, 16–24 Hz), θ (θ1, 4–5 Hz; θ2, 6–7 Hz), and δ (δ, 1 –3 Hz) can be employed to analyze the fatigue states and for fatigue evaluation. In this paper, the four algorithms are compared with each other and the best one is identified.

2.   Materials and Methods

Analog filters are restricted by component tolerances and aging, which results in incorrect measurements.[12] Thus, we use digital filters. Some applications of digital filters must operate in real time. This places specific requirements on the digital signal processor (DSP) depending on the sampling frequency and filter complication. Although DSP processors are fast, their high cost is a real concern. Fortunately, a DSP processor can be ignored when EEG signals can be sent through a USB interface to a personal computer in this system since the program can replace the chip, and a personal computer (PC) is available everywhere.

The sampling frequency for EEG is not high. According to the Nyquist-Shannon theorem, the sampling frequency is at least two times larger than the signal bandwidth. However, in medical field applications, a sampling rate of 8 to 12 times of the signal bandwidth is required. Therefore, we chose an analog-to-digital converter (ADC) with a sampling rate of 500 Hz.

With the calculated differential and average values resulting from measurement by twos in any close time, plus comparison among the variance of four algorithms, the most suitable algorithm is identified.

Subjective ratings of sleepiness are obtained using a version of KSS. The KSS scale consists of a nine-point scale with verbal descriptions for each step (Akerstedt & Gillberg;[2] Gillberg *et al.*[13]). Steps 1, 3, 5, 7, and 9 contain a verbal description of drowsiness. It was modified by Horne and Reyner,[14] who added verbal descriptions to intermediate steps, which did not have any descriptions in the original version, and the modified version of KSS is shown in Table 1.

2.1   *Measurement system*

We use electrode pads as sensing elements. We stick the pads above the frontal bone, which is equivalent to 10–20 international standard of electrode placement at the position of Fz. As indicated in the upper right corner of Fig. 2(a), the positions of the electrode pads are shown.

The block diagram of the proposed system in our state detector is shown in Figs. 2(a) and 2(b). The employed sensors are noninvasive electrode pads and the sensed signals are sent to an amplifier (IA, instrument amplifier) with a suitable gain. The low-pass-filter circuit removes the artificial pseudosignal to obtain the EEG signal, and then converts the signal into a microcontroller by a photocoupler. The photocoupler can protect humans against electric shock. The microcontroller sends the ADC data (EEG data) to a PC by USB. Finally, the data through the digital filter of 200 taps by a PC is divided into various bands, which are analyzed to identify fatigue states.

Table 1
Modified version of KSS.

Rate	Verbal descriptions
1	Extremely alert
2	Very alert
3	Alert
4	Fairly alert
5	Neither alert nor sleepy
6	Some signs of sleepiness
7	Sleepy, but no effort to keep alert
8	Sleepy, some effort to keep alert
9	Very sleepy, great effort to keep alert, fighting sleep
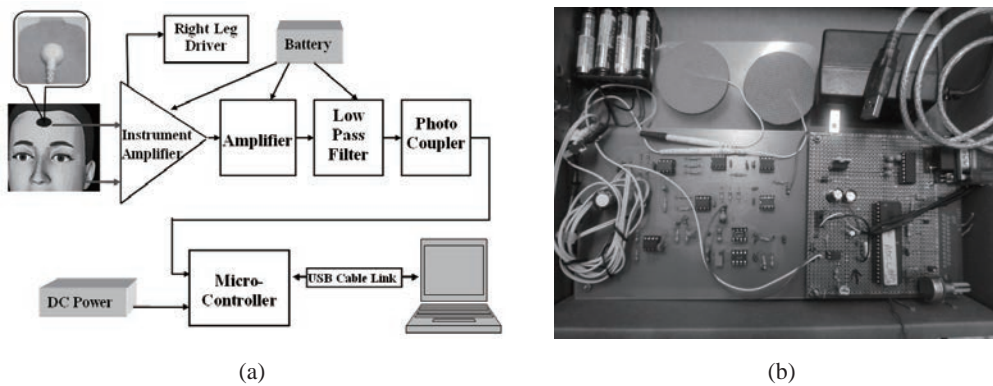
Fig. 2. (a) Block diagram of measurement system and (b) photo of prototype and sensors.

The implemented circuits are shown in Figs. 3(a) and 3(b), which includes a front-end circuit and a microcontroller. The front-end circuit includes an instrument amplifier with a suitable gain, a filter, and a photocoupler. The microcontroller circuit includes a microcontroller and a USB interface.

2.2 *Mode and algorithm*

The microcontroller converts the EEG analog signals into digital with a sampling rate of 500 Hz, and then the data is sent to a PC. This microcontroller features a 10-bit successive approximation ADC.

The PC would store the digitalized data. A finite-impulse response (FIR) band-pass filter is used to divide the energy zone of α1, α2, β1, β2, θ1, θ2, and δ wave bands. Each digital filter has 200 taps of Raised Cosine (other types are Rectangular, Bartlett, Hanning, Hamming, Blackman, Blackman-Harris, Kaiser, Dolph-Cheby and Root Raised Cos). According to our experience, this type is suitable for those bands. Equation (1) defines the finite convolution of an FIR filter.
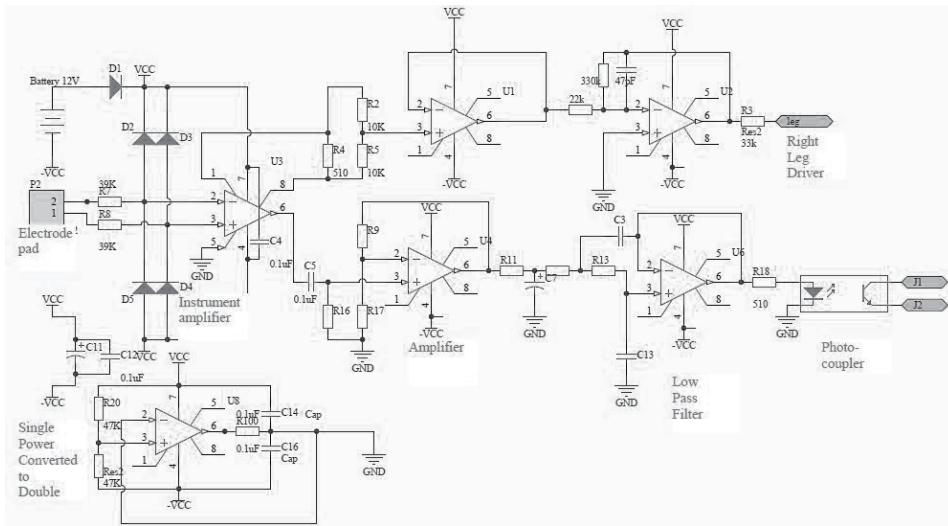
(a)
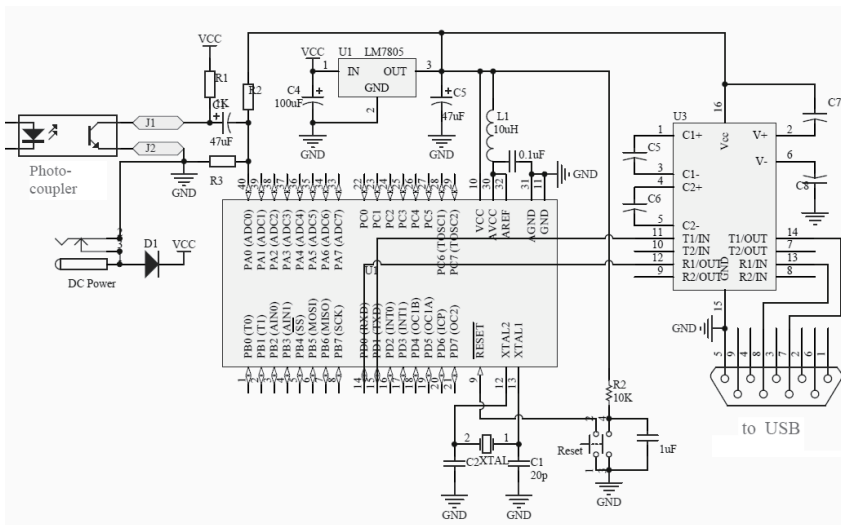
(b)

Fig. 3. (a) Front-end circuit and (b) microcontroller circuit.

$$y(i) = h(i) * x(i) = \sum_{k=0}^{N-1} h(k)x(i-k) \tag{1}$$

Here, x is the input sequence to a filter, y is the filtered sequence, h is the FIR filter coefficient and $N(200)$ is the number of taps.

We make use of the Filter Solutions Toolkit to solve each band value of $x(0)$ to $x(199)$ ($N = 200$). In this case, the $y(i)$ value ($i = 0$ to 2047) is solved with a Visual Basic program using a sampling rate of 500 Hz and time interval of 4.096 s.

The subprograms of each band are shown as follows:

```
    double  y_a1(in_var, is_init)
    {   static float delay [200] = {0,0,0,0,0,0,0,0,0,0,....................................};
        static float x[200] = {1.25e-03,2.307e-04, -8.096e-04,-1.838e-03,-2.822e-03
                         ,.............................. ,-2.822e-03,-1.838e-03, -8.096e-04
                             ,2.307e-04,1.25e-03};
      if (is_init==1)
      {  for (i=0;i<=199;i++) delay[i] = 1.001*in_var;
         return 0.0;
      }
       else
      {  summum=0.0;
         for (i=0;i<=198;i++)
         {   delay[i] = delay[i+1];
             summum += delay[i]*x [i];
         }
         delay[199] = in_var;
         summum += delay[199]*x [199];
         return summum;
      }
    }
```

Power energy of each band (α, β, θ, and δ) was calculated using eq. (2),

$$P_\kappa = \sum_{i=1}^{n} (\kappa(i))^2, \kappa = \alpha, \beta, \theta, \text{ or } \delta, \tag{2}$$

where n is the total number of data ($n = 2048$) and $\kappa(i)$ is the band of the filtered sequence data array.

2.3   *Data analysis*

Table 2 lists the power energy band ratios for 19 different frequencies. Each band power ratio was calculated by dividing the absolute power in the frequency band by the total power, and multiplying this by 100. We input 1 to 19 frequencies with a 60 Hz aliasing signal to verify the correctness of the system. In the results, digital filters provide such good discrimination of bands that analog filters are unable to compete. Since the bandwidth is narrow in analog circuits, the accuracy will be seriously affected by the precision of each component. Particularly with a capacitor of less than 1% accuracy, it is very difficult to achieve.

Table 3 shows the variance of the data. Since $F = 0.141562 < F (0.05, 4, 45) = 2.578739$, it has failed to reject H0 (null hypothesis). Moreover, the *p*-value is 0.965793, which shows 96.5793% probability and has no significant difference.

The operation of the system is shown in Fig. 4. The lower left of the diagram shows the values obtained from the four algorithms.

Table 2
Power energy band ratios. Values are percentages (numbers).

	Wave				
	δ	θ	α	β1	β2
Hz	1–3	4–7	8–12	13–15	16–24
1	57.5 (%)	15.5	21.2	5	0.5
2	58.4	18.6	18.3	4.3	0
5	5.3	91.6	2.5	0.3	0
6	14.6	80.6	3.9	0.7	0
9	2.6	1.8	95	0.4	0
11	2.3	1.9	95.3	0.2	0
13	1.9	1.6	12.5	83.4	0.3
15	1.8	1.3	4.8	81.1	10.7
17	1.1	0.7	1.4	1	95.6
19	0.8	0.4	0.5	0.2	97.8

Note: Unit of band power ratio is percentage.

Table 3
ANOVA (α = 0.05 level of significance).

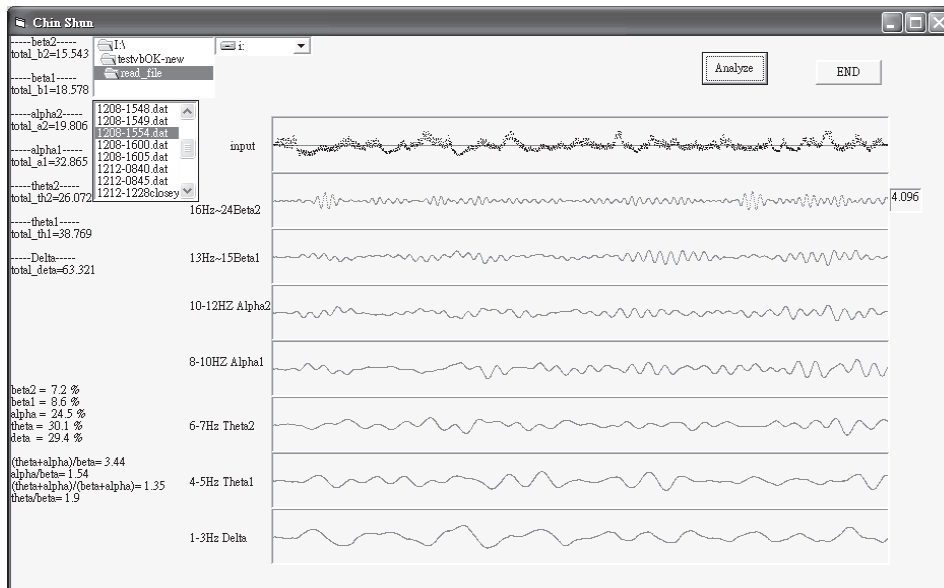| Sources of variation	*SS*	*df*	*MS*	*F*	*P*	Critical value
Between groups	671.8852	4	167.9713	0.141562	0.965793	2.578739
Within groups	53395.14	45	1186.559			
Total	54067.02	49				

Fig. 4.   Operation of system on a PC.

3. Results

The records of repeated measurements in different times using the distance and average value between any two closest times are shown in Table 4. After the one-way analysis of variance (ANOVA) processing, the results by distance are shown in Table 5, and by average shown in Table 6. If the variance of distance is smaller, algorithm 3 is the smallest, which has high precision. The average can determine the correlation between each other.

Table 6 presents the result of $F = 14.099921 > 3.098391$ (critical value); it means that there is enough evidence to tell the differences between these four algorithm variances. That is, they are not in accordance at all. Table 7 presents the results from paired sample correlations; algorithms 3 and 4 have significant correlation ($0.000 < \alpha = 0.05$) and positive correlation; algorithms 1 and 3 have significant correlation ($0.013 < \alpha = 0.05$) and positive correlation; algorithms 1 and 4 have significant correlation ($0.002 < \alpha = 0.05$) and positive correlation. Thus, no significant differences were found at algorithms 1, 3, and 4. Algorithm 2 is different from the other three.

4. Discussion

In the fields of science, engineering, industry, and statistics, the accuracy of a measurement system is the degree of closeness of measurements of a quantity to that quantity's actual value. Data analysis is shown in Table 2, which reveals that the separation and accuracy of the band energy are sufficient. Figure 5 is shown using the input 9 Hz with 60 Hz aliasing signals. It can be found that the alpha band achieves 95%, which means that it has the same accuracy. Input 15 Hz with 60 Hz aliasing signals can be found showing that the beta band reaches 91.8%. Input 5 Hz with 60 Hz aliasing signals can be found showing that the theta band is 91.6%.

Table 4
Fatigue statuses measured at different times.

Date: time	Algorithm 1	Distance	Algorithm 2	Distance	Algorithm 3	Distance	Algorithm 4	Distance
1208:1321	5.81	0.08	2.29	0.47	1.76	0.2	3.52	0.39
1208:1322	5.89		2.76		1.56		3.13	
1208:1536	3.59	0.19	2.01	0.08	1.19	0.1	1.57	0.28
1208:1538	3.78		1.93		1.29		1.85	
1208:1548	5.11	1.15	1.31	0.91	2.21	0.27	3.8	0.24
1208:1549	6.26		2.22		1.94		4.04	
1208:1600	4.9	0.3	2.05	0.47	1.6	0.18	2.85	0.16
1208:1605	4.6		1.58		1.78		3.01	
1212:0840	3.26	2.48	1.47	0.5	1.31	0.62	1.78	1.99
1212:0845	5.74		1.97		1.93		3.77	
1212:1228	1.99	1.04	1.04	0.8	0.97	0.09	0.95	0.23
1212:1229	3.03		1.84		1.06		1.18	

Table 5
Summary of distance between any two closest times.

Group	Number	Sum	Mean	Variance	Std. error mean	Standard deviation
Algorithm 1	6	5.240000	0.873333	0.822147	0.370168	0.906723
Algorithm 2	6	3.230000	0.538333	0.085497	0.119371	0.292398
Algorithm 3	6	1.460000	0.243333	0.038507	0.080111	0.196231
Algorithm 4	6	3.290000	0.548333	0.504537	0.289982	0.710307

Table 6
ANOVA of average between any two closest times.

Sources of variation	Sum of squares	*df*	*MS*	*F*	*P*	Critical value
Between groups	31.347808	3	10.449269	14.099921	0.000036	3.098391
Within groups	14.821742	20	0.7410870			
Total	46.169550	23				

Table 7
Paired samples correlations.

		N	Correlation	Sig.
Pair 1	Algorithm 1 & algorithm 2	6	0.665023	0.149520
Pair 2	Algorithm 1 & algorithm 3	6	0.905522	0.012967
Pair 3	Algorithm 1 & algorithm 4	6	0.966317	0.001683
Pair 4	Algorithm 2 & algorithm 3	6	0.292014	0.574429
Pair 5	Algorithm 2 & algorithm 4	6	0.450428	0.370051
Pair 6	Algorithm 3 & algorithm 4	6	0.981870	0.000490

Fig. 5. Input 9 Hz with 60 Hz aliasing signals. The α band there can be found to achieve 95%.

The precision of a measurement system, also called reproducibility or repeatability, is the degree to which repeated measurements under unchanged conditions show the same results. If repeated measurements are conducted in nearest times and the results of each are very close, the precision is high. When the four types of algorithm are checked, algorithm 3 has the smallest variance (see Table 5) and has a positive correlation with algorithms 1 and 4. Therefore, we consider that algorithm 3 being equal to $(\theta+\alpha)/(\alpha+\beta)$ is the best choice.

5.   Conclusions

Only two electrode pads are employed in our system, and they are portable and can be easily and quickly installed without using complex electrodes.

Our system is proved to be portable, accurate, and precise as shown in algorithm 3. Rapid and noninvasive measurement allows high acceptance and good user acceptances within less than 15 min of measurement at a time. On the other hand, the detection of anxiety ($\beta2$ moving to the right side) can help doctors judge and evaluate psychotropic drugs.

References

1   J. A. Horne and S. D. Baulk: Psychophysiology **41** (2004) 161.
2   T. Akerstedt and M. Gillberg: Int. J. Neurosci. **52** (1990) 29.
3   M. S. Arjena, G. M. B. Domien, D. Berdine, H. Nynke and D. Serge: Neurosci. Lett. **340** (2003) 17.
4   W. Miroslaw, K. Jan and M. L. C. Anton: Acta Neurobiol. Exp. **68** (2008) 180.
5   B. A. Edelstein: Clinical Geropsycholog: Comprehensive Clinical Psychology vol. 7 (Pergamon, Amsterdam, 2001) p. 182.
6   M. Ansseau, A. Doumont, J. L. Cerfointaine, H. Mantanus, J. C. Rousseau and B. M. Timsit: Neuropsychobiology **12** (1984) 255.
7   T. Isotani, H. Tanaka, D. Lehmann, R. D. Pascual-Marqui, K. Kochi, N. Saito, T. Yagyu, T. Kinoshita and K. Sasada: Int. J. Psychophysiol. **41** (2001) 143.
8   E. Niedermayer and F. H. Lopes: Electroencephalography: Basic Principles, Clinical Applications, and Related Fields, 1st ed. (Lippincott, Williams & Wilkins, Philadelphia, 1999) p. 1098.
9   K. A. Brookhuis and D. Waard: Ergonomics **39** (1993) 1099.
10   H. J. Eoh, M. K. Chung and S. H. Kim: Int. J. Ind. Ergon. **35** (2005) 307.
11   J. T. Budi, L. Sara, F. Peter and B. Evangelos: Expert Syst. Appl. **36** (2009) 2352.
12   G. W. Greenwood: Instrum. Sci. Tech. **22** (1994) 313.
13   M. Gillberg, G. Kecklund and T. Akerstedt: Sleep **17** (1994) 236.
14   J. A. Horne and L. A. Reyner: Br. Med. J. **310** (1995) 565.